Bioengineering

Research article

Enhancing public health strategies for tungiasis: A mathematical approach with fractional derivative

Norliyana Nor Hisham Shah[1]**, Rashid Jan**[1]**, Hassan Ahmad**[2]**, Normy Norfiza Abdul Razak**[1]**, Imtiaz Ahmad**[3,*]**and Hijaz Ahmad**[4,*]

[1] Institute of Energy Infrastructure (IEI), Department of Civil Engineering, College of Engineering, Universiti Tenaga Nasional (UNITEN), Putrajaya Campus, Jalan IKRAM-UNITEN, 43000 Kajang, Selangor, Malaysia

[2] Department of Mathematics, University of Swabi, Swabi 23561, KPK, Pakistan

[3] Institute of Informatics and Computing in Energy (IICE), Universiti Tenaga Nasional, Kajang, Selangor, Malaysia

[4] Section of Mathematics, International Telematic University Uninettuno, Corso Vittorio Emanuele II, 39,00186 Roma, Italy

* **Correspondence:** Email: imtiazkakakhil@gmail.com; ahmad.hijaz@uninettuno.it.

Abstract: In this study, we formulate a mathematical model in the framework of the Atangana-Baleanu fractional derivative in Caputo sense to study the transmission of tungiasis. In this formulation, interactions between the human host and the sand fleas are taken into consideration, including factors like infestation rate, incubation duration, and recovery rate. We calculate the basic reproduction parameter for the system, symbolized by $\mathcal{R}_0$ with the help of the next-generation matrix technique. A novel numerical scheme for encapsulating the non-local and memory-dependent aspects of the system is conceptualized via the Atangana-Baleanu fractional derivative. We prove the existence and uniqueness of the solution of the model of the infection and establish stability of the steady-states of the model. In addition to this, numerical simulations are carried out to evaluate the efficiency of interventions like campaigns for better sanitation and treatment, and to investigate the influence of various management techniques on the prevalence of tungiasis. The outcomes of the numerical simulations give us information about the possible efficacy of different control strategies in lowering the incidence of tungiasis. This research gives quantitative tools to enhance decision-making processes in public health treatments and advances our understanding of the dynamics of the tungiasis.

Keywords: tungiasis; mathematical model; endemic indicator; Atangan-Baleanu derivative; fixed point theory; time series analysis

1. Introduction

Tungiasis is a parasitic skin condition brought on by female sand fleas and is sometimes referred to as jiggers or sand flea infestation. Tropical and subtropical regions, especially the regions of America, Asia, Africa and the Caribbean, are infected with this disease. The flea enters into the skin, usually in areas where the skin is thin, such as the toes, heels and the spaces between toes and fingers [1]. The female sand flea burrows into the skin and grows into a small, swollen, and painful lesion, often resembling a tiny white or black dot. The flea then lays eggs inside this lesion and after development to complete the life cycle. The primary symptom of tungiasis is intense itching, leading to scratching, which can cause secondary bacterial infections. The affected area may become red, swollen, and painful. Over time, the lesions may grow larger and more uncomfortable [2]. Tungiasis is usually diagnosed based on clinical signs and symptoms. The presence of a specific lesion in the toes or feet, especially in areas with a history of sand flea infestations, helps with diagnosis [3]. The most effective treatment for tungiasis is the removal of the embedded sand fleas using sterilized instruments or a needle. The lesion should be cleaned and disinfected to prevent infections. In severe cases, topical antibiotics may be prescribed if secondary infections have developed [4]. Preventive measures include avoiding walking barefoot in sandy or contaminated areas and wearing protective footwear.

Surgical extraction of embedded sand fleas under sterile medical conditions [5] can also be considered an efficacious therapeutic approach for its management. Tungiasis is a preventable condition, but it can cause significant discomfort and complications if left untreated [6]. If you suspect you have tungiasis or are experiencing symptoms, it is essential to seek medical attention for proper diagnosis and treatment. The infected areas often experience subpar living conditions and inadequate sanitation, making the inhabitants particularly susceptible to the infestation [7]. The afflicted populations face serious health and economical difficulties as a result of this neglected tropical illness. The mechanics of tungiasis transmission must be understood in order to adopt effective control measures and lessen the disease's effects. Jiggers, chigoe flea infection, and pulex penetrans infestation are a few of the historical names for tungiasis [8]. The female sand flea that transmits the disease burrows into the skin, concentrating on the feet, causing painful sores, inflammatory reactions, and secondary infections if left untreated.

Mathematical models have significantly contributed to enhancing comprehension of the fundamental mechanisms of biological processes for public health [9–15]. Over the years, researchers and public health experts have dedicated significant efforts to gain insight into the spread of various infections [16]. Previous research has concentrated on a variety of disease-related topics [17, 18], from clinical symptoms and epidemiology to control methods and therapies. The frequency and geographic distribution of tungiasis have been examined in studies, revealing insight on the disease's burden and its effects on afflicted people [19, 20]. Kahuru et al conducted a study focused on employing an optimal control approach within a mathematical model to analyze the dynamics of tungiasis within a community [21]. The researchers in [22] established the stability results of the transmission dynamics of the disease. After that, the theory of optimal control is utilized, all with the ultimate goal of reducing the numbers of infested humans, infested animals, and sand flea populations [23]. The processes of disease transmission and the potential effects of interventions like better sanitation, health education, and treatment campaigns have both benefited greatly from these modeling studies [24]. Mathematical modeling of infectious diseases enhances our understanding of

the diseases, facilitates evidence-based decision-making, and helps implement targeted interventions to reduce the burden of the condition in affected communities. In this work, we will enhance our scientific comprehension of tungiasis dynamics to provide more valuable perspectives for efficient management approaches. Through the utilization of mathematical modeling and simulation methods, we will evaluate the prospective consequences of treatments and facilitate decision-making within the realm of public health to improve the effectiveness of interventions and control measures.

Fractional calculus is a branch of mathematics that deals with derivatives and integrals of non-integer orders. It extends the concepts of traditional calculus, which involves integer-order derivatives and integrals. Fractional calculus has found applications in various scientific fields [25–30], including epidemiology, where it can be used to model the spread of infectious diseases. It has been acknowledged that fractional calculus offers a more flexible framework for describing complex real-world problems [31, 32]. The Atangana-Baleanu fractional derivative is a type of fractional derivative that has been applied to various mathematical models, including epidemic models [33, 34]. Fractional calculus generalizes the concept of traditional derivatives and integrals to non-integer orders, allowing for a more flexible representation of complex phenomena, such as anomalous diffusion or power-law behaviors [35]. In the context of epidemic models, the Atangana-Baleanu fractional derivative has been utilized to introduce memory effects and long-range interactions into the system. In addition to this, these models can capture more realistic scenarios and provide insights into the long-term behavior of infectious diseases. Hence, we choose to represent the dynamics of tungiasis using a fractional framework to obtain more precise results.

This article is organized as follows: The fundamental concepts and results of the fractional theory related to the ABC operator is presented in Section 2. In Section 3, we formulated a mathematical model for tungiasis through the ABC operator in the fractional framework. In Section 4, the suggested model is subsequently examined. In Section 5, the solution of the recommended model is investigated with the help of fixed-point theory. Then, we introduced a numerical scheme to highlight the dynamical behaviour of the system in Section 6. Finally, ending remarks of the work are presented with future work in Section 7.

2. Preliminaries of fractional-calculus

The main relevant findings and definitions of classical Caputo [36] and Atangana-Baleanu fractional derivatives [37] will be presented here and will be useful in the following portion of the paper.

Definition 2.1. *Let* $f : [p, q] \rightarrow \mathbb{R}$ *be a given function, then the fractional derivative of Caputo fractional derivative of order* $\jmath$ *is given by*

$$\,_p^C D_t^{\jmath}(u(t)) = \frac{1}{\Gamma(n - \jmath)} \int_p^t u^n(\kappa)(t - \kappa)^{n - \jmath - 1} d\kappa,$$

for $\jmath \in (n - 1, n)$*, where* $n \in \mathbf{Z}$*.*

Definition 2.2. *The Atangana-Beleanu fractional derivative for a given function* f *in the Caputo form is introduced as*

$$\,_p^{ABC} D_t^{\jmath} f(t) = \frac{B(\jmath)}{1 - \jmath} \int_p^t f'(\kappa) E_{\jmath} \left[-\jmath \frac{(t - \kappa)^{\jmath}}{1 - \jmath} \right] d\kappa,$$

where $f \in H^1(p, q)$, $q > p$, and $J \in [0, 1]$. In addition to this, $B(J)$ is the normalization function which satisfies the condition $B(0) = B(1) = 1$.

Definition 2.3. *The integral of the ABC derivative is denoted by ${}^{ABC}_p I^J_t f(t)$ and is defined as:*

$$
{}^{ABC}_p I^J_t f(t) = \frac{1 - J}{B(J)} f(t) + \frac{J}{B(J)\Gamma(J)} \int_p^t f(\kappa)(t - \kappa)^{J-1} d\kappa.
$$

Theorem 2.1. *Assume f in a manner that $f \in C[p, q]$, then we have the equation below mentioned in [37]:*

$$
\|{}^{ABC}_p D^J_t(f(t))\| < \frac{B(J)}{1 - J} \|f(t)\|, \; where \; \|f(t)\| = max_{p \leq t \leq q}|f(t)|.
$$

Furthermore, it has been established that ABC derivatives satisfy the Lipschitz condition [37].

$$
\|{}^{ABC}_p D^J_t f_1(t) - {}^{ABC}_p D^J_t f_2(t)\| < \vartheta_1 \|f_1(t) - f_2(t)\|.
$$

3. Evaluation of the dynamics

Here we present a mathematical model of Tungiasis disease. In this approach, the total population is divided into four categories: group that practices good hygiene ($\mathcal{P}$), susceptible ($\mathcal{S}$), infected ($\mathcal{I}$), and treated ($\mathcal{T}$) groups. Then, the total population is

$$
\mathcal{N}(t) = \mathcal{P}(t) + \mathcal{S}(t) + \mathcal{I}(t) + \mathcal{T}(t).
$$

At birth, the population that is most susceptible is recruited at a rate of $(1 - \gamma)\upsilon$, whereas the group that practices good hygiene is recruited at $\gamma\upsilon$ where υ represents the rate of recruitment at birth and γ represents the likelihood of being recruited into the category of good hygiene practices. The appropriate hygiene practice group ($\mathcal{P}$) develops susceptibility ($\mathcal{S}$) at a rate of φ. Individuals from the class ($\mathcal{S}$) move to the class ($\mathcal{I}$) with a rate Γ. The infected individuals ($\mathcal{I}$) transfer to the treated group ($\mathcal{T}$) at a rate of ϱ following therapy. We indicated the natural death rate by μ. The infection rate Γ is defined as

$$
\Gamma = \frac{\sigma \varepsilon \mathcal{I}}{\mathcal{N}},
$$

where ε is the contact rate with infected people and σ is the likelihood of being infected after repeated exposure to infected people. Then our model with the above assumptions for tungiasis disease is as follows:

$$
\begin{cases}
\frac{d\mathcal{P}}{dt} &= \gamma\upsilon - (\varphi + \mu)\mathcal{P}, \\
\frac{d\mathcal{S}}{dt} &= (1 - \gamma)\upsilon + \varphi\mathcal{P} - (\Gamma + \mu)\mathcal{S}, \\
\frac{d\mathcal{I}}{dt} &= \Gamma\mathcal{S} - (\omega + \varrho + \mu)\mathcal{I}, \\
\frac{d\mathcal{T}}{dt} &= \varrho\mathcal{I} - \mu\mathcal{T},
\end{cases}
\tag{3.1}
$$

with appropriate initial condition

$$
\mathcal{P}(0) > 0, \; \mathcal{S}(0) > 0, \; \mathcal{I}(0) > 0, \; \mathcal{T}(0) > 0.
\tag{3.2}
$$

Table 1. Parameter values with interpretation used in the proposed system.

Parameter	Interpretation
γ	Probability of recruitment in $\mathcal{P}(t)$
υ	Birth or recruitment rate
φ	The losing rate of protection
μ	Death occurs naturally in each class
Γ	Infection rate from susceptible to infected class
ω	Disease induced mortality rate
ϱ	Treatment rate for the infection
σ	Rate of transmission of the infection
ε	Contact rate of infection

It is acknowledged that epidemic models through the Atangana-Baleanu fractional derivative can more accurately represents the dynamics of infectious diseases than conventional integer derivatives. This inclusion enables a more comprehensive exploration of epidemic spread in intricate settings characterized by long-range interactions and memory effects, fostering an improved comprehension of the underlying mechanisms. Consequently, the refined insights gained from these fractional derivative-based models hold the potential to enhance the precision of epidemic predictions and facilitate the development of more efficacious control strategies. Nonetheless, it is crucial to acknowledge that the introduction of fractional derivatives into mathematical models may introduce increased system complexity, necessitating the utilization of specialized mathematical and numerical techniques for rigorous analysis and simulation. Thus, the model (3.1) recommended above can be written in fractional form as

$$
\begin{cases}
{}^{ABC}_{0}D_t^J\mathcal{P} &= \gamma\upsilon - (\varphi + \mu)\mathcal{P}, \\
{}^{ABC}_{0}D_t^J\mathcal{S} &= (1 - \gamma)\upsilon + \varphi\mathcal{P} - (\Gamma + \mu)\mathcal{S}, \\
{}^{ABC}_{0}D_t^J\mathcal{I} &= \Gamma\mathcal{S} - (\omega + \varrho + \mu)\mathcal{I}, \\
{}^{ABC}_{0}D_t^J\mathcal{T} &= \varrho\mathcal{I} - \mu\mathcal{T}.
\end{cases}
\tag{3.3}
$$

All of the parameters in the recommended model (3.1) for tungiasis disease are considered to be positive. Furthermore, the term ${}^{ABC}_{0}D_t^J$ in the above model indicates the ABC derivative. The effects of memory which arise in the epidemiological process but are not incorporated in the classical operators, are the driving force behind fractional order models. In Table 1, we illustrated the parameters of the recommended model with description.

4. Analysis of the model

In this section, we deal with some analysis of the model, like steady-state analysis, and find the basic reproduction ratio $\mathcal{R}_0$ for the above model (3.3). As the system (3.3) models the population of humans, all state variable solutions with nonnegative beginning conditions are nonnegative $\forall t > 0$ and have a feasible region bound as follows:

$$
\Xi = \left((\mathcal{P}, \mathcal{S}, \mathcal{I}, \mathcal{T}) \in \mathbb{R}_+^4; \mathcal{S}, \mathcal{P}, \mathcal{I}, \mathcal{T} \geq 0; \mathcal{N} \leq \frac{\upsilon}{\mu} \right).
$$

In the upcoming step, we will focus on the steady-states of the suggested system of the infection. First, we take the following:

$$_{0}^{ABC}D_{t}^{J}\mathcal{P} =_{0}^{ABC}D_{t}^{J}\mathcal{S} =_{0}^{ABC}D_{t}^{J}\mathcal{I} =_{0}^{ABC}D_{t}^{J}\mathcal{T} = 0,$$

then, the model (3.3) becomes

$$\begin{cases} 0 & = & \gamma\upsilon - (\varphi + \mu)\mathcal{P}, \\ 0 & = & (1 - \gamma)\upsilon + \varphi\mathcal{P} - (\Gamma + \mu)\mathcal{S}, \\ 0 & = & \Gamma\mathcal{S} - (\omega + \varrho + \mu)\mathcal{I}, \\ 0 & = & \varrho\mathcal{I} - \mu\mathcal{T}. \end{cases} \tag{4.1}$$

The disease-free equilibrium of an epidemic model refers to a stable state where the infectious disease has been eliminated from the population. Understanding the disease-free equilibrium is essential in assessing the effectiveness of control strategies and vaccination programs. It serves as a benchmark to measure the success of public health interventions in eliminating or controlling infectious diseases and preventing outbreaks. For the infection-free steady-state, we set

$$\mathcal{P} = \mathcal{P}^{o}, \mathcal{S} = \mathcal{S}^{o}, \mathcal{I} = \mathcal{I}^{o}, \mathcal{T} = \mathcal{T}^{o} \ and \ \mathcal{N} = \mathcal{N}^{o}.$$

Thus, we have

$$E_{o} = (\mathcal{P}^{o}, \mathcal{S}^{o}, \mathcal{I}^{o}, \mathcal{T}^{o}) = \left(0, \frac{(1 - \gamma)\upsilon}{(\Gamma + \mu)}, 0, 0\right).$$

The endemic equilibrium (EE) of an epidemic model refers to a stable state where the prevalence of the infectious disease remains constant over time. Understanding the endemic equilibrium of an epidemic model is crucial in assessing the long-term behavior of the infection and evaluating the quality of control measures in maintaining the disease at a manageable level. It provides valuable insights into the stability and persistence of the infection in a population and is a fundamental concept in the study of infectious disease dynamics. We indicate the EE of the system by (E^{*}) and substitute $\Gamma = \frac{\sigma\varepsilon\mathcal{I}}{\mathcal{N}}$. Then from (4.1), we have

$$\begin{cases} 0 & = & \gamma\upsilon - (\varphi + \mu)\mathcal{P}^{*}, \\ 0 & = & (1 - \gamma)\upsilon + \varphi\mathcal{P}^{*} - \left(\frac{\sigma\varepsilon\mathcal{I}^{*}}{\mathcal{N}^{*}} + \mu\right)\mathcal{S}^{*}, \\ 0 & = & \frac{\sigma\varepsilon\mathcal{I}^{*}}{\mathcal{N}^{*}}\mathcal{S}^{*} - (\omega + \varrho + \mu)\mathcal{I}^{*}, \\ 0 & = & \varrho\mathcal{I}^{*} - \mu\mathcal{T}^{*}. \end{cases} \tag{4.2}$$

Solving the above system (4.2), we have

$$E^{*}\begin{pmatrix} \mathcal{P}^{*} \\ \mathcal{S}^{*} \\ \mathcal{I}^{*} \\ \mathcal{T}^{*} \end{pmatrix} = E^{*}\begin{pmatrix} \frac{\gamma\upsilon}{\varphi+\mu} \\ \frac{\mathcal{N}^{*}(\omega+\varrho+\mu)}{\sigma\varepsilon} \\ \frac{1}{(\omega+\varrho+\mu)}\left[\frac{(\varphi-\gamma\mu+\mu)\upsilon}{(\varphi+\mu)} - \frac{\mathcal{N}^{*}\mu(\omega+\varrho+\mu)}{\sigma\varepsilon}\right] \\ \frac{\varrho}{\mu(\omega+\varrho+\mu)}\left[\frac{(\varphi-\gamma\mu+\mu)\upsilon}{(\varphi+\mu)} - \frac{\mathcal{N}^{*}\mu(\omega+\varrho+\mu)}{\sigma\varepsilon}\right] \end{pmatrix}.$$

The basic reproduction number is a fundamental concept in epidemiology that quantifies the potential of an infection to spread. It represents the average number of secondary infections generated by a single infected individual in a fully susceptible environment. If the basic reproduction number is less than 1, it means that, on average, each infected individual will cause fewer than one new infection

during their infectious period. In this case, the disease will not be able to sustain itself in the population, and it will eventually die out. If this parameter is equal to 1, this implies that, on average, each infected individual will cause exactly one new infection during their infectious period. The disease will reach a stable endemic equilibrium, where the number of new infections is balanced by the number of recoveries, resulting in a constant prevalence of the disease in the population. If this parameter is greater than 1, this implies that each infected individual, on average, will cause more than one new infection during their infectious period. In this case, the disease has the potential to spread, and if left uncontrolled, it may lead to an epidemic outbreak.

We symbolized this number as $\mathcal{R}_0$ and calculate it through the next-generation matrix method [38]. We take the infected class of the system (3.1), so we have

$$\,^{ABC}_{0}D^J_t \mathcal{I} = \Gamma\mathcal{S} - (\omega + \varrho + \mu)\,\mathcal{I}. \tag{4.3}$$

Let F be the matrix containing parameters that are entering into infected class and V be the matrix containing those parameters that leave infected classes while neglecting the negative signs, so we get

$$F = \Gamma\mathcal{S} = \frac{\sigma\varepsilon\mathcal{I}\mathcal{S}}{\mathcal{N}},$$

and

$$V = (\omega + \varrho + \mu)\,\mathcal{I}.$$

This implies that $\mathcal{R}_0 = \dfrac{\sigma\varepsilon}{\omega + \varrho + \mu}$, which is the required $\mathcal{R}_0$ of the recommended system.

Theorem 4.1. *For $J = 1$, the infection-free steady-state E_0 of the system (3.3) is locally asymptotically stable if $\mathcal{R}_0 < 1$, otherwise it is unstable.*

Proof. Let $J = 1$ and take the Jacobian matrix of the model (3.3) at infection-free steady-state E_0 as

$$\mathfrak{J}(E_o) = \begin{bmatrix} -(\varphi + \mu) & 0 & 0 & 0 \\ \varphi & -\left(\frac{\sigma\varepsilon\mathcal{I}^o}{\mathcal{N}} + \mu\right) & -\frac{\sigma\varepsilon\mathcal{I}^o}{\mathcal{N}} & 0 \\ 0 & \frac{\sigma\varepsilon\mathcal{I}^o}{\mathcal{N}} & \frac{\sigma\varepsilon\mathcal{S}^o}{\mathcal{N}} - (\varrho + \omega + \mu) & 0 \\ 0 & 0 & \varrho & -\mu \end{bmatrix}.$$

The above Jacobian matrix has the following characteristic equation:

$$|\mathfrak{J}(E_o) - \lambda I| = 0,$$

furthermore, we have

$$\begin{vmatrix} -(\varphi + \mu) - \lambda & 0 & 0 & 0 \\ \varphi & -\left(\frac{\sigma\varepsilon\mathcal{I}^o}{\mathcal{N}} + \mu\right) - \lambda & -\frac{\sigma\varepsilon\mathcal{I}^o}{\mathcal{N}} & 0 \\ 0 & \frac{\sigma\varepsilon\mathcal{I}^o}{\mathcal{N}} & \frac{\sigma\varepsilon\mathcal{S}^o}{\mathcal{N}} - (\varrho + \omega + \mu) - \lambda & 0 \\ 0 & 0 & \varrho & -\mu - \lambda \end{vmatrix} = 0,$$

and simplifying, we have

$$(-(\varphi + \mu) - \lambda) \begin{vmatrix} -\left(\frac{\sigma\varepsilon\mathcal{I}^o}{\mathcal{N}} + \mu\right) - \lambda & -\frac{\sigma\varepsilon\mathcal{I}^o}{\mathcal{N}} & 0 \\ \frac{\sigma\varepsilon\mathcal{I}^o}{\mathcal{N}} & \frac{\sigma\varepsilon\mathcal{S}^o}{\mathcal{N}} - (\varrho + \omega + \mu) - \lambda & 0 \\ 0 & \varrho & -\mu - \lambda \end{vmatrix} = 0,$$

which implies that $\lambda_1 = -(\varphi + \mu)$ and

$$\begin{vmatrix} -\left(\frac{\sigma\varepsilon I^o}{N} + \mu\right) - \lambda & -\frac{\sigma\varepsilon I^o}{N} & 0 \\ \frac{\sigma\varepsilon I^o}{N} & \frac{\sigma\varepsilon S^o}{N} - (\varrho + \omega + \mu) - \lambda & 0 \\ 0 & \varrho & -\mu - \lambda \end{vmatrix} = 0,$$

the simplification of which implies that

$$(-\mu - \lambda)\begin{vmatrix} -\left(\frac{\sigma\varepsilon I^o}{N} + \mu\right) - \lambda & -\frac{\sigma\varepsilon I^o}{N} \\ \frac{\sigma\varepsilon I^o}{N} & \frac{\sigma\varepsilon S^o}{N} - (\varrho + \omega + \mu) - \lambda \end{vmatrix} = 0.$$

From the above, we have $\lambda_2 = -\mu$ and

$$\begin{vmatrix} -\left(\frac{\sigma\varepsilon I^o}{N} + \mu\right) - \lambda & -\frac{\sigma\varepsilon I^o}{N} \\ \frac{\sigma\varepsilon I^o}{N} & \frac{\sigma\varepsilon S^o}{N} - (\varrho + \omega + \mu) - \lambda \end{vmatrix} = 0$$

Hence, all the eigen values are negative. Furthermore, we have $\mathcal{J}_1(E_0)$ given by

$$\mathcal{J}_1(E_0) = \begin{bmatrix} -\left(\frac{\sigma\varepsilon I^o}{N} + \mu\right) & -\frac{\sigma\varepsilon I^o}{N} \\ \frac{\sigma\varepsilon I^o}{N} & \frac{\sigma\varepsilon S^o}{N} - (\varrho + \omega + \mu) \end{bmatrix} = 0.$$

To show the required result, we have to show that $\text{Tace}(\mathcal{J}_1(E_o)) < 0$ and $\text{Det}(\mathcal{J}_1(E_o)) > 0$, so

$$Trace(\mathcal{J}_1(E_o)) = -\left(\frac{\sigma\varepsilon I^o}{N} + \mu\right) + \frac{\sigma\varepsilon S^o}{N} - (\varrho + \omega + \mu),$$

$$= -\mu + \sigma\varepsilon - (\varrho + \omega + \mu),$$

$$= -\mu + \sigma\varepsilon - \varrho - \omega - \mu,$$

$$= -2\mu + \sigma\varepsilon - (\varrho + \omega),$$

$$Trace(\mathcal{J}_1(E_0)) = -(2\mu - \sigma\varepsilon + (\varrho + \omega)) < 0,$$

which implies that

$$Trace(\mathcal{J}_1(E_o)) < 0.$$

Also, we have

$$Det(\mathcal{J}_1(E_0)) = \begin{vmatrix} -\left(\frac{\sigma\varepsilon I^o}{N} + \mu\right) & -\frac{\sigma\varepsilon I^o}{N} \\ \frac{\sigma\varepsilon I^o}{N} & \frac{\sigma\varepsilon S^o}{N} - (\varrho + \omega + \mu) \end{vmatrix}$$

$$= \left[-\left(\frac{\sigma\varepsilon I^o}{N} + \mu\right)\left(\frac{\sigma\varepsilon S^o}{N} - (\varrho + \omega + \mu)\right) - \left(-\frac{\sigma\varepsilon I^o}{N}\right)\left(\frac{\sigma\varepsilon I^o}{N}\right)\right].$$

Because $\mathcal{R}_0 < 1$ is given, so the Det will be positive, that is, $Det(\mathcal{J}_1(E_0)) > 0$. Hence, the infection-free steady-state of the recommended system is locally asymptotically stable (LAS) for $\mathcal{R}_0 < 1$ and unstable in other cases.

Theorem 4.2. *For $\jmath = 1$, the endemic steady-state (E^*) of system (3.3) is LAS if $\mathcal{R}_0 > 1$ and is unstable in other circumstances.*

Proof. Let $J = 1$ and take the Jacobian matrix of system (3.3) at endemic steady-state (E^*) as

$$\mathfrak{J}(E)^* = \begin{bmatrix} -(\varphi + \mu) & 0 & 0 & 0 \\ \varphi & -\left(\frac{\sigma\varepsilon I^*}{N^*} + \mu\right) & -\frac{\sigma\varepsilon I^*}{N^*} & 0 \\ 0 & \frac{\sigma\varepsilon I^*}{N^*} & \frac{\sigma\varepsilon S^*}{N^*} - (\varrho + \omega + \mu) & 0 \\ 0 & 0 & \varrho & -\mu, \end{bmatrix},$$

furthermore, we get

$$\mathfrak{J}(E^*) = \begin{bmatrix} -(\varphi + \mu) & 0 & 0 & 0 \\ \varphi & -\left(\frac{\sigma\varepsilon W}{N^*} + \mu\right) & -\frac{\sigma\varepsilon W}{N^*} & 0 \\ 0 & \frac{\sigma\varepsilon W}{N^*} & -(\varrho + \omega + \mu) & 0 \\ 0 & 0 & \varrho & -\mu, \end{bmatrix},$$

in which $W = \frac{1}{(\omega+\varrho+\mu)}\left[\frac{(\varphi-\gamma\mu+\mu)\upsilon}{(\varphi+\mu)} - \frac{N^*\mu(\omega+\varrho+\mu)}{\sigma\varepsilon}\right]$. The characteristic equation is $(\varphi + \mu + \lambda)(\mu + \lambda)\left[\lambda^2 + \left(\frac{\sigma\varepsilon W}{N^*} + \mu\right)\lambda + \frac{\sigma\varepsilon(\omega+\varrho+\mu)W}{N^*}\right] = 0$, which implies that $\lambda_1 = -(\varphi + \mu)$ and $\lambda_2 = -\mu$ with the following

$$\lambda^2 + \left(\frac{\sigma\varepsilon W}{N^*} + \mu\right)\lambda + \frac{\sigma\varepsilon(\omega + \varrho + \mu)W}{N^*} = 0. \tag{4.4}$$

Substituting the value of W into (4.4), we get

$$\lambda^2 + m\lambda + n = 0, \tag{4.5}$$

in which $m = \frac{\mathcal{R}_o((\varphi-\gamma\mu+\mu)\upsilon)}{(\varphi+\mu)N^*}$ and $n = \frac{\sigma\varepsilon(\varphi-\gamma\mu+\mu)\upsilon}{(\varphi+\mu)N^*} - (\omega + \varrho + \mu)\mu$. Hence it is clear that $m, n > 1$, also $\mathcal{R}_0 = \frac{\sigma\varepsilon}{\omega+\varrho+\mu} > 1$. The eigenvalues provided by equation (4.5) are negative according to the Routh-Hurwitz criteria. Thus, whenever $\mathcal{R}_0 > 1$, the EE of the proposed model of tungiasis is locally asymptotically stable.

5. Fractional order model solution

In this section of the paper, we utilize fixed point theory to demonstrate the existence and uniqueness of the fractional order model (3.3) solution. The system of equations can be represented in the following way:

$$\begin{cases} {}^{ABC}_0 D^J_t s(t) = \mathcal{U}(t, v(t)), \\ v(0) = v_0, \quad 0 < t < T < \infty. \end{cases} \tag{5.1}$$

In the above (5.1), $v(t) = (\mathcal{P}, \mathcal{S}, \mathcal{I}, \mathcal{T})$ is the vector form of the state variables and $\mathcal{U}$ is a continuous vector function. Moreover, $\mathcal{U}$ is given by

$$\mathcal{U} = \begin{pmatrix} \mathcal{U}_1 \\ \mathcal{U}_2 \\ \mathcal{U}_3 \\ \mathcal{U}_4 \end{pmatrix} = \begin{pmatrix} \gamma\upsilon - (\varphi + \mu)\mathcal{P}, \\ (1 - \gamma)\upsilon + \varphi\mathcal{P} - (\Gamma + \mu)\mathcal{S}, \\ \Gamma\mathcal{S} - (\omega + \varrho + \mu)\mathcal{I}, \\ \varrho\mathcal{I} - \mu\mathcal{T} \end{pmatrix},$$

and $v_0(t) = (\mathcal{P}(0), \mathcal{S}(0), \mathcal{I}(0), \mathcal{T}(0))$ are initial conditions. In addition to this, the Lipschitz condition is fulfilled by $\mathcal{U}$ as

$$\|\mathcal{U}(t, v_1(t)) - \mathcal{U}(t, v_2(t))\| \leq \mathcal{N}\|v_1(t) - v_2(t)\|. \tag{5.2}$$

In the upcoming step, the existence and uniqueness of the fractional order dynamical model (3.3) will be proved.

Theorem 5.1. *The solution of fractional order (FO) model of equations (3.3) will be unique if the below mentioned condition satisfies:*

$$\frac{(1 - J)}{ABC(J)}\mathcal{N} + \frac{J}{ABC(J)\Gamma(J)}T_{max}^{J}\mathcal{N} < 1. \tag{5.3}$$

Proof. In order to demonstrate the desired result, we utilize the Atangana-Beleanu (AB) fractional integral, as defined in (2.3), on system (5.1). This yields a non-linear Volterra integral equation as follows:

$$v(t) = v_0 + \frac{1 - J}{ABC(J)}\mathcal{U}(t, r(t)) + \frac{J}{ABC(J)\Gamma(J)}\int_0^t (t - \kappa)^{J-1}\mathcal{U}(\kappa, v(\kappa))d\kappa. \tag{5.4}$$

Take $I = (0, T)$ and the operator $\Phi : \mathcal{G}(I, R^4) \to \mathcal{G}(I, R^4)$ defined by

$$\Phi[v(t)] = v_0 + \frac{1 - J}{ABC(J)}\mathcal{U}(t, v(t)) + \frac{J}{ABC(J)\Gamma(J)}\int_0^t (t - \kappa)^{J-1}\mathcal{U}(\kappa, v(\kappa))d\kappa. \tag{5.5}$$

Equation (5.4) takes the following form

$$v(t) = \Phi[v(t)], \tag{5.6}$$

and the supremum norm on I is indicated by $\|.\|_I$ and is

$$\|v(t)\|_I = \sup_{t \in I} \|v(t)\|, \quad v(t) \in \mathcal{G}. \tag{5.7}$$

Certainly, $\mathcal{G}(I, R^4)$ with norm $\|.\|_I$ becomes a Banach space and

$$\left\| \int_0^t \mathcal{F}(t, \kappa)v(\kappa)d\kappa \right\| \leq T\|\mathcal{F}(t, \kappa)\|_I\|v(t)\|_I, \tag{5.8}$$

with $v(t) \in \mathcal{G}(I, R^4)$, $\mathcal{F}(t, \kappa) \in \mathcal{G}(I^2, R)$ in a manner that

$$\|\mathcal{F}(t, \kappa)\|_I = \sup_{t,\kappa \in I} |\mathcal{F}(t, \kappa)|. \tag{5.9}$$

Here, utilizing the definition of Φ shown in (5.6), we have

$$\|\Phi[v_1(t)] - \Phi[v_2(t)]\|_I \leq \left\| \frac{(1 - J)}{ABC(J)}(\mathcal{U}(t, v_1(t)) - \mathcal{U}(t, v_2(t)) + \frac{J}{ABC(J)\Gamma(J)} \times \right.$$
$$\left. \int_0^t (t - \kappa)^{J-1}(\mathcal{U}(\kappa, v_1(\kappa)) - \mathcal{U}(\kappa, v_2(\kappa)))d\kappa \right\|_I \tag{5.10}$$

Additionally, by applying the Lipschitz condition (5.2) and the triangular inequality, in combination with the result in (5.8), we arrive at the below expression after simplification:

$$\|\Phi[v_1(t)] - \Phi[v_1(t)]\|_I \leq \left(\frac{(1-j)\mathcal{N}}{ABC(j)} + \frac{j}{ABC(j)\Gamma(j)} \mathcal{N}T_{max}^j \right) \|v_1(t) - v_2(t)\|_I. \tag{5.11}$$

Consequently, we have the following:

$$\|\Phi[v_1(t)] - \Phi[v_1(t)]\|_I \leq B\|v_1(t) - v_2(t)\|_I, \tag{5.12}$$

in which

$$B = \frac{(1-j)\mathcal{N}}{ABC(j)} + \frac{j}{ABC(j)\Gamma(j)} \mathcal{N}T_{max}^j.$$

It is evident that when condition (5.3) is met, Φ becomes a contraction, implying that the fractional order dynamical system (5.1) possesses a unique solution.

6. Iterative scheme and results

In this section, we will present an iterative scheme for the numerical solution of the recommended model (3.3) of the infection. First, an iterative scheme will be developed and then the the solution pathways of the system will be represented through the scheme to understand the dynamics. We use the newly established numerical approach (iterative) proposed for the approximation of the AB integral operator [39]. We briefly describe and apply the aforesaid approach to our dynamical system (3.3) in order to show the impact of different parameters on the infection.

Here, rewriting system (5.4) of the infection into the fractional integral equation form using the fundamental theorem of fractional calculus:

$$s(t) - s(0) = \frac{(1-j)}{ABC(j)} \mathcal{U}(t, s(t)) + \frac{j}{ABC(j) \times \Gamma(j)} \int_0^t \mathcal{U}(\kappa, x(\xi))(t-\kappa)^{j-1} d\xi. \tag{6.1}$$

At $t = t_{\xi+1}$, $\xi = 0, 1, 2, ...$, we have

$$\begin{aligned} s(t_{\xi+1}) - s(0) &= \frac{1-j}{ABC(j)} \mathcal{U}(t_\xi, s(t_\xi)) + \\ &\quad \frac{j}{ABC(j) \times \Gamma(j)} \int_0^{t_{\xi+1}} \mathcal{U}(\kappa, s(\kappa))(t_{\xi+1} - \kappa)^{j-1} dj, \\ &= \frac{1-j}{ABC(j)} \mathcal{U}(t_\xi, s(t_\xi)) + \\ &\quad \frac{j}{ABC(j) \times \Gamma(j)} \sum_{j=0}^{\xi} \int_{t_j}^{t_{j+1}} \mathcal{U}(\kappa, s(\kappa))(t_{\xi+1} - \kappa)^{j-1} dj. \end{aligned} \tag{6.2}$$

The function $\mathcal{U}(\kappa, s(\kappa))$ can be estimated over the interval $[t_j, t_{j+1}]$, and we apply the interpolation polynomial

$$\mathcal{U}(\kappa, s(\kappa)) \cong \frac{\mathcal{U}(t_j, s(t_j))}{h}(t - t_{j-1}) - \frac{\mathcal{U}(t_{j-1}, s(t_{j-1}))}{h}(t - t_j), \tag{6.3}$$

then substituting in (6.2), we get

$$
\begin{aligned}
s(t_{\xi+1}) \;=\; & s(0) + \frac{1-J}{ABC(J)}\mathcal{U}(t_\xi, s(t_\xi)) + \frac{J}{ABC(J)\times\Gamma(J)} \\
& \sum_{j=0}^{\xi}\Big(\frac{\mathcal{U}(t_j, s(t_j))}{h}\int_{t_j}^{t_{j+1}}(t-t_{j-1})(t_{\xi+1}-t)^{J-1}dt \\
& -\frac{\mathcal{U}(t_{j-1}, s(t_{j-1}))}{h}\int_{t_j}^{t_{j+1}}(t-t_j)(t_{\xi+1}-t)^{J-1}dt\Big).
\end{aligned} \tag{6.4}
$$

After computing these integrals, the approximate answer is as follows:

$$
\begin{aligned}
s(t_{\xi+1}) \;=\; & s(t_0) + \frac{1-J}{ABC(J)}\mathcal{U}(t_\xi, s(t_\xi)) + \frac{J}{ABC(J)}\sum_{j=0}^{\xi} \\
& \Big(\frac{h^J\mathcal{U}(t_j, s(t_j))}{\Gamma(J+2)}((\xi+1-j)^J(\xi-j+2+J)-(\xi-j)^J(\xi-j+2+2J)) \\
& -\frac{h^J\mathcal{U}(t_{j-1}, s(t_{j-1}))}{\Gamma(J+2)}((\xi+1-j)^{J+1}-(\xi-j)^J(\xi-j+1+J))\Big).
\end{aligned} \tag{6.5}
$$

Finally, for the suggested model, we achieved the following recursive formulae:

$$
\begin{aligned}
\mathcal{P}(t_{\xi+1}) \;=\; & \mathcal{P}(t_0) + \frac{1-J}{ABC(J)}\mathcal{U}_1(t_\xi, s(t_\xi)) + \frac{J}{ABC(J)}\sum_{j=0}^{\xi} \\
& \Big(\frac{h^J\mathcal{U}_1(t_j, s(t_j))}{\Gamma(J+2)}((\xi+1-j)^J(\xi-j+2+J)-(\xi-j)^J(\xi-j+2+2J)) \\
& -\frac{h^J\mathcal{U}_1(t_{j-1}, s(t_{j-1}))}{\Gamma(J+2)}((\xi+1-j)^{J+1}-(\xi-j)^J(\xi-j+1+J))\Big) \\[6pt]
\mathcal{S}(t_{\xi+1}) \;=\; & \mathcal{S}(t_0) + \frac{1-J}{ABC(J)}\mathcal{U}_2(t_\xi, s(t_\xi)) + \frac{J}{ABC(J)}\sum_{j=0}^{k} \\
& \Big(\frac{f^J\mathcal{U}_2(t_j, s(t_j))}{\Gamma(J+2)}((\xi+1-j)^J(\xi-j+2+J)-(\xi-j)^J(\xi-j+2+2J)) \\
& -\frac{h^J\mathcal{U}_2(t_{j-1}, s(t_{j-1}))}{\Gamma(J+2)}((\xi+1-j)^{J+1}-(\xi-j)^J(\xi-j+1+J))\Big) \\[6pt]
\mathcal{I}(t_{\xi+1}) \;=\; & \mathcal{I}(t_0) + \frac{1-J}{ABC(J)}\mathcal{U}_3(t_\xi, s(t_\xi)) + \frac{J}{ABC(J)}\sum_{j=0}^{\xi} \\
& \Big(\frac{h^J\mathcal{U}_3(t_j, s(t_j))}{\Gamma(J+2)}((\xi+1-j)^J(\xi-j+2+J)-(\xi-j)^J(\xi-j+2+2J)) \\
& -\frac{h^J\mathcal{U}_3(t_{j-1}, s(t_{j-1}))}{\Gamma(J+2)}((\xi+1-j)^{J+1}-(\xi-j)^J(\xi-j+1+J))\Big) \\[6pt]
\mathcal{T}(t_{\xi+1}) \;=\; & \mathcal{T}(t_0) + \frac{1-J}{ABC(J)}\mathcal{U}_4(t_\xi, s(t_\xi)) + \frac{J}{ABC(J)}\sum_{j=0}^{\xi}
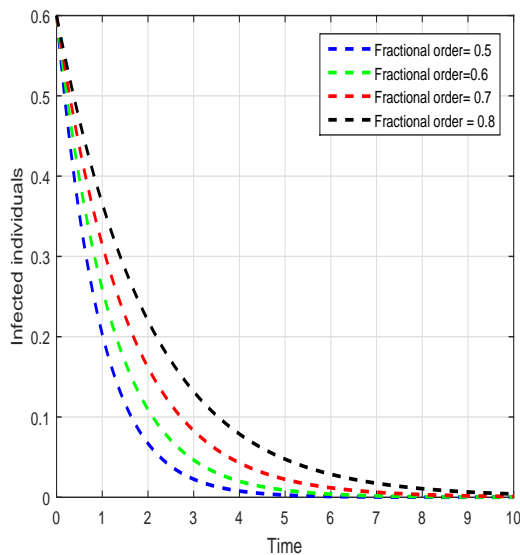\end{aligned}
$$

$$\Big(\frac{f^J\mathcal{U}_4(t_j, s(t_j))}{\Gamma(J+2)}((\xi+1-j)^J(\xi-j+2+j) - (\xi-j)^J(\xi-j+2+2j))$$

$$-\frac{f^J\mathcal{U}_4(t_{j-1}, s(t_{j-1}))}{\Gamma(J+2)}((n+1-j)^{J+1} - (\xi-j)^J(\xi-j+1+j))\Big). \tag{6.6}$$
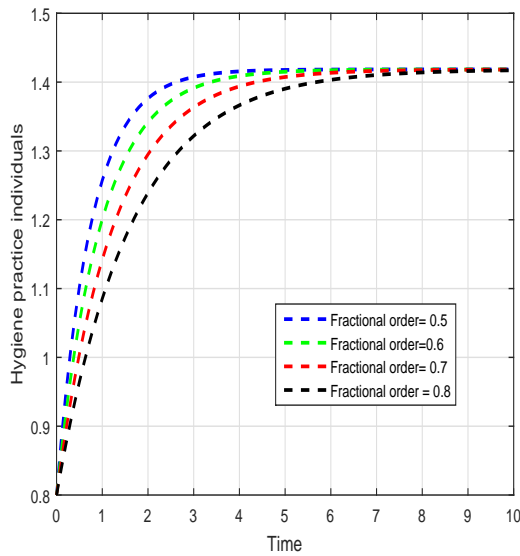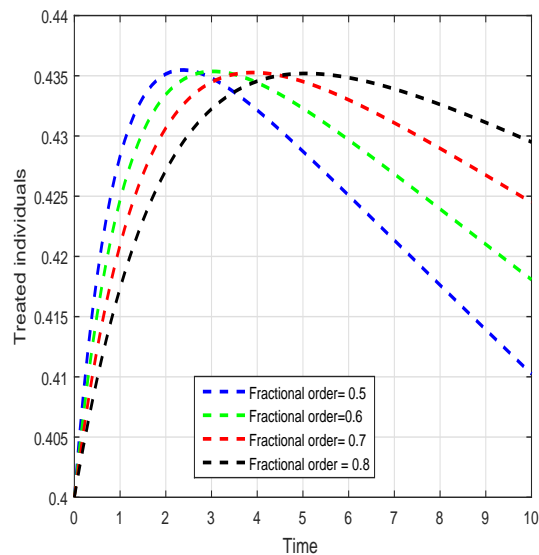

(a)
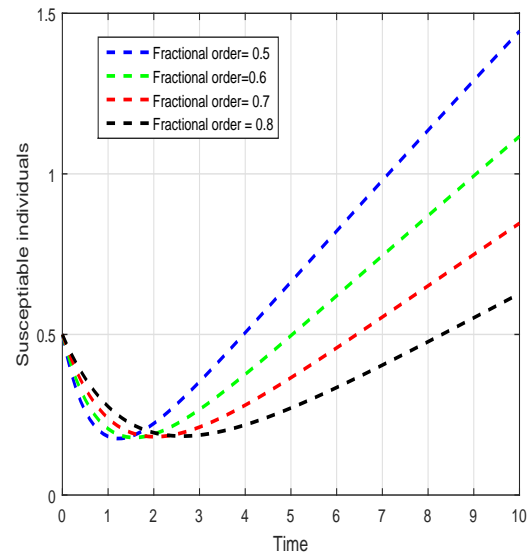
(b)

(c)

(d)

Figure 1. Visualization of the tracking path behavior of the suggested model under varying fractional parameter values J, i.e., $J = 0.5, 0.6, 0.7, 0.8$.
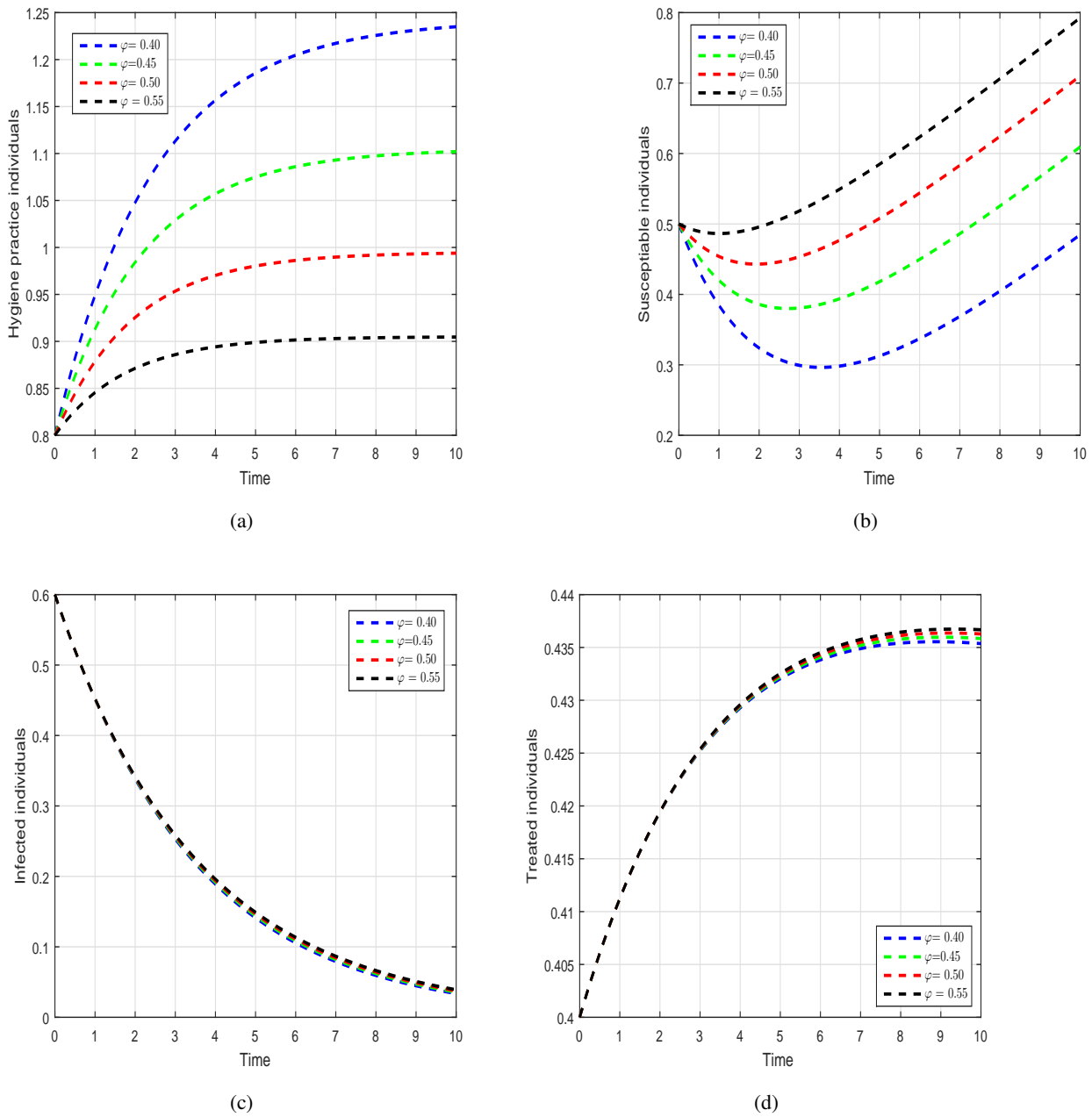
Figure 2. Illustration of the solution pathways of the suggested model with varying values of the losing rate of protection φ, i.e., $\varphi = 0.40, 0.45, 0.50, 0.55$.
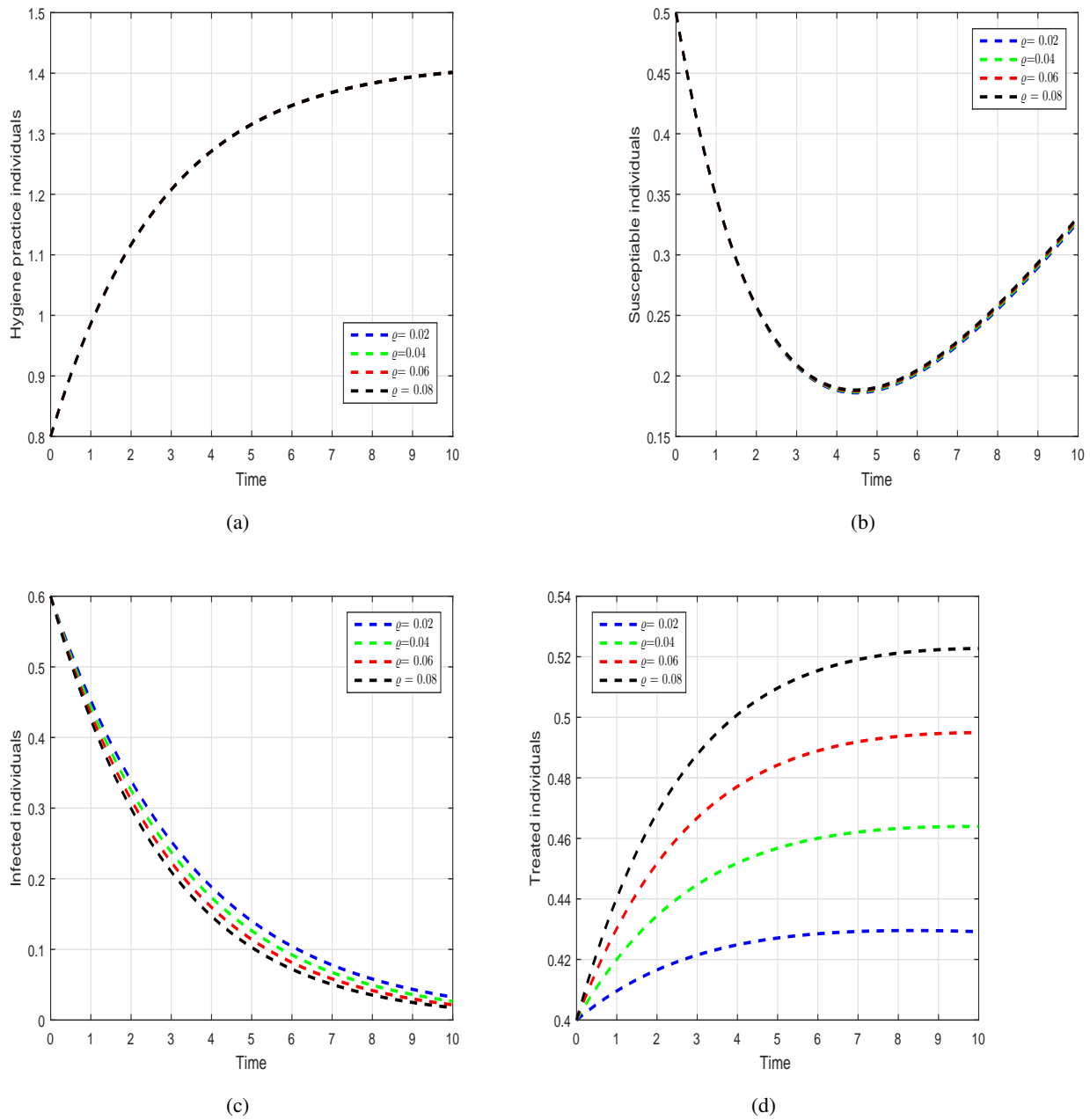
Figure 3. Illustration of the solution pathways of the suggested model with varying values of the treatment rate ϱ, i.e., $\varrho = 0.02, 0.04, 0.06, 0.08$.
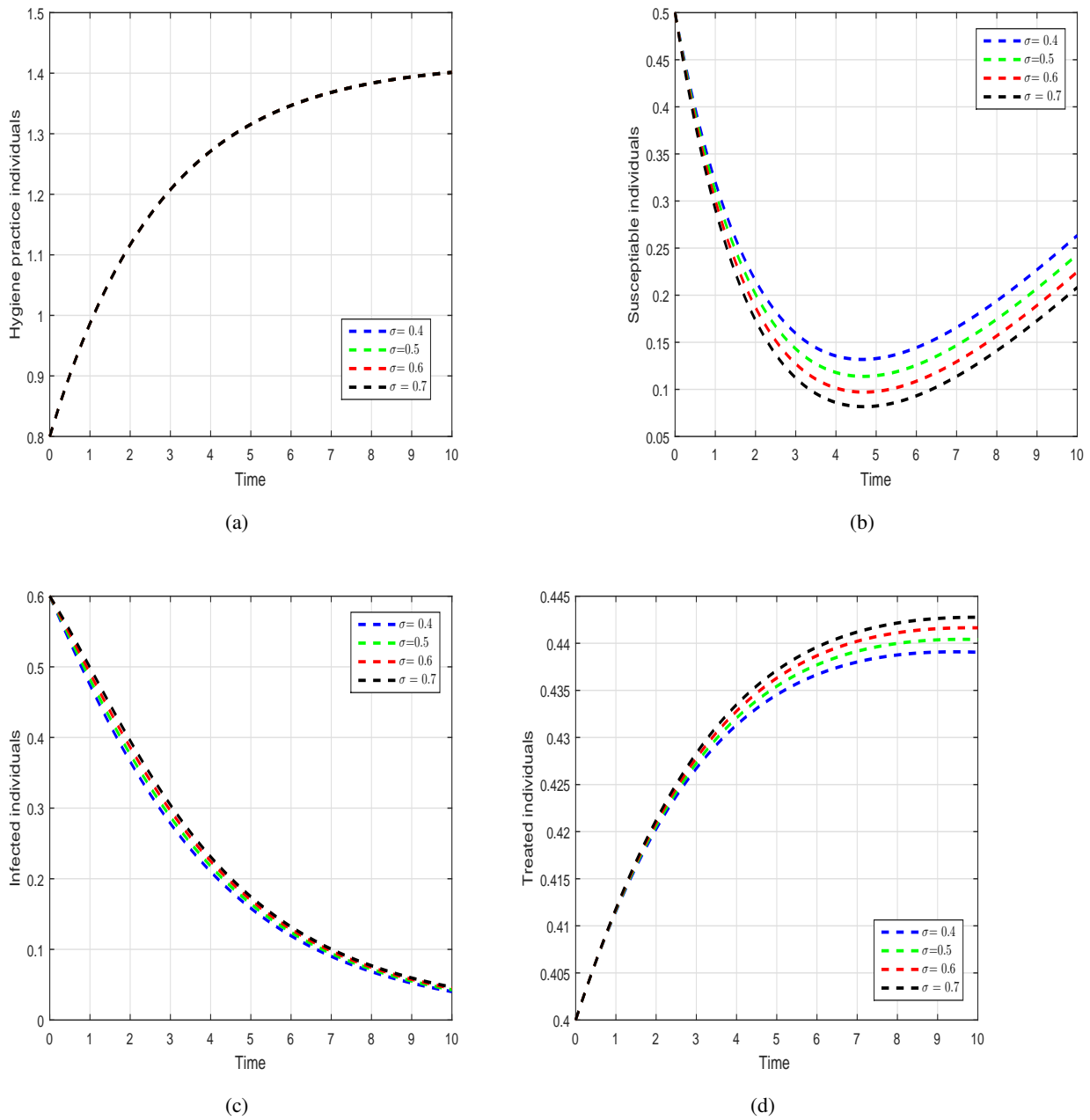
(a)

(b)

(c)

(d)

Figure 4. Representing the time series of the class of the proposed system of the infection with varying values of the transmission probability σ, i.e., $\sigma = 0.40, 0.50, 0.60, 0.70$.
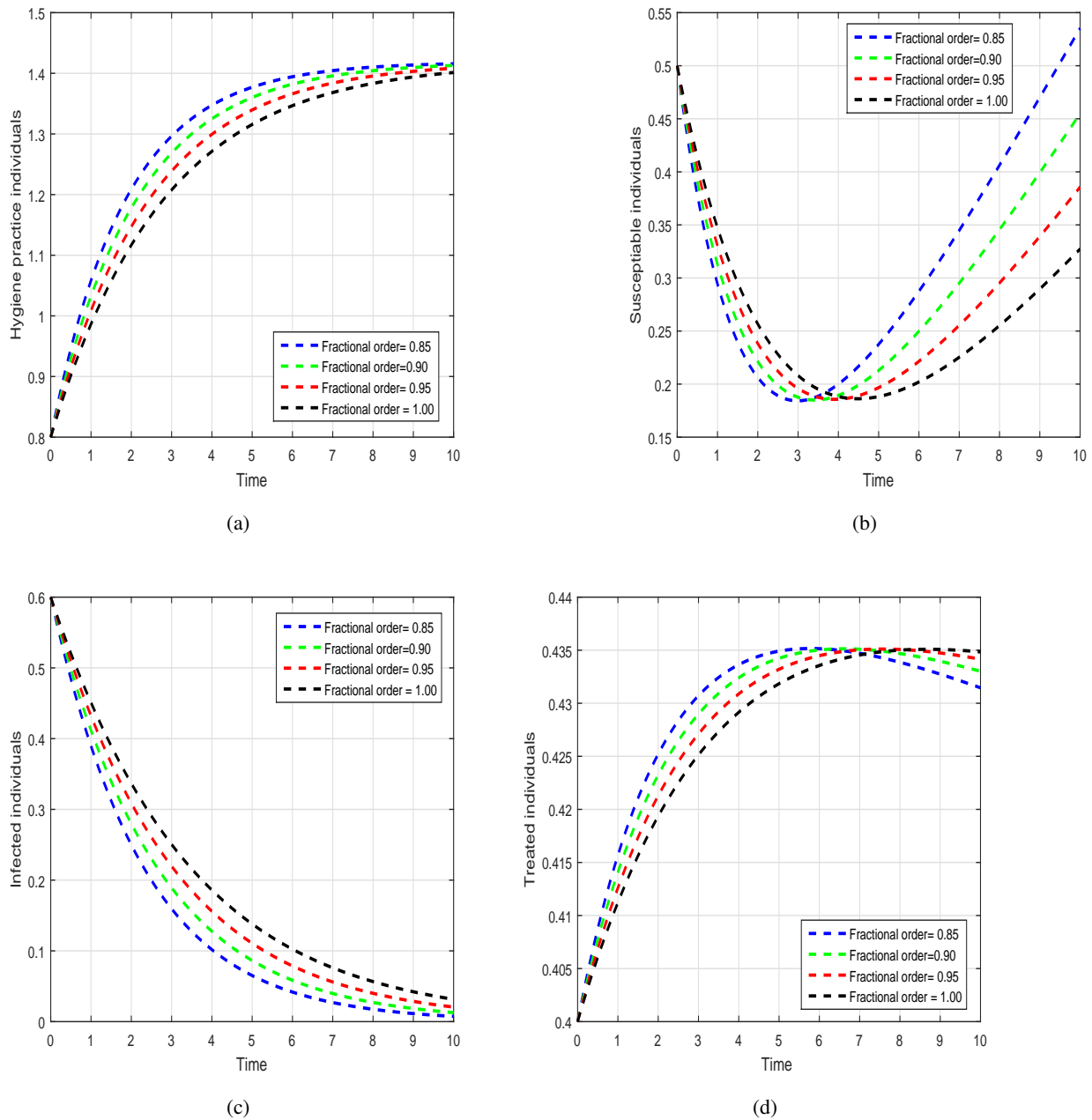
Figure 5. Visualization of the tracking path behavior of the suggested model under varying fractional parameter values $\jmath$, i.e., $\jmath = 0.85, 0.90, 0.95, 1.00$.

We will utilize the above alterative approach to investigate the dynamical behaviour of the recommended fractional model of tungiasis. It is well-known that the graphical view analysis of epidemic models provide a comprehensive exploration of the model's behavior, leading to a better understanding of the epidemic's spread and potential control strategies. Here, we will perform different simulations to visualize the impact of different input factors on the system.

The values of the input parameter and state variables of the system are assumed for numerical purposes. For our investigation, we conducted a series of simulations to analyze the behavior of the

system under different conditions. In these simulations, we varied specific parameters and observed their impact on the solution pathways of the system. First, in Figure 1 and Figure 5, we examined the effect of the fractional parameter $\jmath$ on the dynamics of the system. By changing the fractional order, we aimed to understand its role in shaping the infection spread in the society. Notably, we observed that decreasing the fractional parameter led to a reduction in the infection rate within the community. This finding indicates that the fractional parameter can serve as a crucial control parameter for managing the epidemic. In Figure 2, we focused on the losing rate of protection and its influence on the dynamics of the tungiasis infection. The results clearly indicate that this parameter plays a pivotal role in determining the risk of infection within the population. A higher losing rate of protection was found to increase the susceptibility to infection, posing a potential threat to public health.

The treatment rate was the primary parameter of interest in Figure 3. By varying the treatment rate ϱ, we explored its impact on the transmission dynamics of the system. The simulation revealed that the treatment rate significantly affects the control of the infection. Higher values of ϱ demonstrated a more effective reduction in infection rates, suggesting its importance in implementing effective intervention strategies. Lastly, Figure 4 focused on understanding the influence of the transmission probability on the tungiasis dynamics. Through this simulation, we visualized how changes in the transmission probability affect the overall dynamics of the infection. The results clearly illustrated that the transmission probability is a critical factor in shaping the infection spread within the community.

Our numerical analysis provided valuable insights into the control and dynamics of tungiasis. The fractional parameter, losing rate of protection, treatment rate, and transmission probability all emerged as significant factors that influence the infection's behavior. In the realm of tungiasis control and intervention, our discovered insights provide a foundational framework for the formulation of effective strategies aimed at managing and mitigating the spread of the infection within affected populations. It is, however, crucial to acknowledge that the values employed in this analysis were assumptions crafted for numerical expediency and may not faithfully replicate real-world scenarios. Consequently, for heightened precision in predictions and practical implications, an imperative next step involves the meticulous validation and refinement of our model using authentic real-world data. This process is indispensable for aligning our theoretical framework with the intricacies of tangible scenarios and enhancing the applicability of our findings in the context of tungiasis control and management.

7. Conclusion

In this study, we formulated an epidemic model for tungiasis disease in the framework of fractional Atangana-Baleanu derivative to conceptualize the transmission route of the infection. The biologically meaningful steady-states of the system are investigated through analytic methods. We determined the basic reproduction number of our fractional model, symbolized by $\mathcal{R}_0$. The existence and uniqueness of the model's solution has been demonstrated. We have shown that the infection-free steady-states of the recommended model are locally asymptotically stable if $\mathcal{R}_0 < 1$ and unstable in other cases, while the endemic steady-state is locally asymptotically stable if $\mathcal{R}_0 > 1$ and unstable in other circumstances. A numerical scheme is presented to illustrate the solution pathways of the recommended system of the infection. The dynamical behaviour of the model is presented with the variation of different input parameters. We recommended the most critical factors of the system for the control and subsequent of

tungiasis. It is acknowledged that delays play a fundamental role in capturing the temporal dynamics of systems [40]. Incorporating delays into mathematical models enhances their predictive power and allows for a more accurate representation of real-world phenomena [41–43]. In the future work, we will incorporate time delay in the transmission dynamics of the disease to comprehend the dynamics of the disease and provide more accurate information for prevention.

Use of AI tools declaration

The authors declare they have not used Artificial Intelligence (AI) tools in the creation of this article.

Acknowledgments

No external funding is used regarding this research.

Conflict of interest

Hijaz Ahmad is on a special issue editorial board for AIMS Bioengineering and was not involved in the editorial review or the decision to publish this article. All authors declare that there are no competing interests. The authors declare that there is no conflict of interests regarding the publication of this paper.

References

1. Feldmeier H, Keysers A (2013) Tungiasis–a Janus-faced parasitic skin disease. *Travel Med Infect Dis* 11: 357–365. https://doi.org/10.1016/j.tmaid.2013.10.001

2. Obebe OO, Aluko OO (2020) Epidemiology of tungiasis in sub-saharan Africa: a systematic review and meta-analysis. *Pathog Glob Health* 114: 360–369. https://doi.org/10.1080/20477724.2020.1813489

3. Chauhan P, Jindal R, Errichetti E (2022) Dermoscopy of skin parasitoses, bites and stings: a systematic review of the literature. *J Eur Acad Dermatol Venereol* 36: 1722–1734. https://doi.org/10.1111/jdv.18352

4. Razanakolona LRS, Raharisoa A, Soankasina AH, et al. (2022) Clinical and epidemiological survey of tungiasis in Madagascar. *J Travel Med* 50: 102449. https://doi.org/10.1016/j.tmaid.2022.102449

5. Feldmeier H, Sentongo E, Krantz I (2013) Tungiasis (sand flea disease): a parasitic disease with particular challenges for public health. *Eur J Clin Microbiol* 32: 19–26. https://doi.org/10.1007/s10096-012-1725-4

6. Campollo MLO, Lievanos SJG, Amparán YIL, et al. (2022) Tungiasis: an underdiagnosed problem. *IJMSCRS* 2: 1484–1486. https://doi.org/10.47191/ijmscrs/v2-i12-23

7. Mutebi F, Krücken J, Feldmeier H, et al. (2021) Clinical implications and treatment options of tungiasis in domestic animals. *Parasitol Res* 120: 4113—4123. https://doi.org/10.1007/s00436-021-07121-y

8. Michael BG, Fikru C, Teka T (2018) Tungiasis: an overview. *J Parasitol Vector Biol* 10: 66–72. https://doi.org/10.5897/JPVB2016.0274

9. Jan R, Khan MA, Kumam P, et al. (2019) Modeling the transmission of dengue infection through fractional derivatives. *Chaos Soliton Fract* 127: 189–216. https://doi.org/10.1016/j.chaos.2019.07.002

10. Tang TQ, Shah Z, Bonyah E, et al. (2022) Modeling and analysis of breast cancer with adverse reactions of chemotherapy treatment through fractional derivative. *Comput Math Methods Med* 2022: 5636844. https://doi.org/10.1155/2022/5636844

11. Li P, Lu Y, Xu C, et al. (2023) Insight into hopf bifurcation and control methods in fractional order BAM neural networks incorporating symmetric structure and delay. *Cogn Comput* 2023: 1–43. https://doi.org/10.1007/s12559-023-10155-2

12. Xu C, Mu D, Pan Y, et al. (2023) Exploring bifurcation in a fractional-order predator-prey system with mixed delays. *J Appl Anal Comput* 13: 1119–1136. https://doi.org/10.11948/20210313

13. Jan R, Boulaaras S (2022) Analysis of fractional-order dynamics of dengue infection with non-linear incidence functions. *Trans Inst Meas Control* 44: 2630–2641. https://doi.org/10.1177/01423312221085049

14. Jan R, Qureshi S, Boulaaras S, et al. (2023) Optimization of the fractional-order parameter with the error analysis for human immunodeficiency virus under Caputo operator. *Discrete Cont Dyn-S* 16: 2118–2140. https://doi.org/10.3934/dcdss.2023010

15. Jan R, Khan A, Boulaaras S, et al. (2022) Dynamical behaviour and chaotic phenomena of HIV infection through fractional calculus. *Discrete Dyn Nat Soc* 2022: 5937420. https://doi.org/10.1155/2022/5937420

16. Alyobi S, Jan R (2023) Qualitative and quantitative qnalysis of fractional dynamics of infectious diseases with control measures. *Fractal Fract* 7: 400. https://doi.org/10.3390/fractalfract7050400

17. Jan R, Shah Z, Deebani W, et al. (2022) Analysis and dynamical behavior of a novel dengue model via fractional calculus. *Int J Biomath* 15: 2250036. https://doi.org/10.1142/S179352452250036X

18. Tang TQ, Shah Z, Jan R, et al. (2022) Modeling the dynamics of tumor–immune cells interactions via fractional calculus. *Eur Phys J Plus* 137: 367. https://doi.org/10.1140/epjp/s13360-022-02591-0

19. Zucconi M, Ferini-Strambi L (2004) Epidemiology and clinical findings of restless legs syndrome. *Sleep Med* 5: 293–299. https://doi.org/10.1016/j.sleep.2004.01.004

20. Eisele M, Heukelbach J, Van Marck E, et al. (2003) Investigations on the biology, epidemiology, pathology and control of Tunga penetrans in Brazil: I. Natural history of tungiasis in man. *Parasitol Res* 90: 87–99. https://doi.org/10.1007/s00436-002-0817-y

21. Kong L, Li L, Kang S, et al. (2022) Dynamic behavior of a stochastic tungiasis model for public health education. *Discrete Dyn Nat Soc* 2022: 4927261. https://doi.org/10.1155/2022/4927261

22. Lv W, Liu L, Zhuang SJ (2022) Dynamics and optimal control in transmission of tungiasis diseases. *Int J Biomath* 15: 2150076. https://doi.org/10.1142/S1793524521500765

23. Kahuru J, Luboobi LS, Nkansah-Gyekye Y (2017) Optimal control techniques on a mathematical model for the dynamics of tungiasis in a community. *Int J Math Math Sci* 2017: 4804897. https://doi.org/10.1155/2017/4804897

24. Feldmeier H, Eisele M, Van Marck E, et al. (2004) Investigations on the biology, epidemiology, pathology and control of Tunga penetrans in Brazil: IV. Clinical and histopathology. *Parasitol Res* 94: 275–282. https://doi.org/10.1007/s00436-004-1197-2

25. Ahmad I, Zaman S (2020) Local meshless differential quadrature collocation method for time-fractional PDEs. *Discrete Cont Dyn-S* 13: 2641–2654. https://doi.org/10.3934/dcdss.2020223

26. Li JF, Ahmad I, Ahmad H, et al. (2020) Numerical solution of two-term time-fractional PDE models arising in mathematical physics using local meshless method. *Open Phys* 18: 1063–1072. https://doi.org/10.1515/phys-2020-0222

27. Wang F, Ahmad I, Ahmad H, et al. (2021) Meshless method based on RBFs for solving three-dimensional multi-term time fractional PDEs arising in engineering phenomenons. *J King Saud Univ Sci* 33: 101604. https://doi.org/10.1016/j.jksus.2021.101604

28. Shakeel M, Khan MN, Ahmad I, et al. (2023) Local meshless collocation scheme for numerical simulation of space fractional PDE. *Therm Sci* 27: 101–109. https://doi.org/10.2298/TSCI23S1101S

29. Almutairi B, Ahmad I, Almohsen B, et al. (2023) Numerical simulations of time-fractional PDEs arising in mathematics and physics using the local Meshless differential quadrature method. *Therm Sci* 27: 263–272. https://doi.org/10.2298/TSCI23S1263A

30. Ahmad H, Khan MN, Ahmad I, et al. (2023) A meshless method for numerical solutions of linear and nonlinear time-fractional Black-Scholes models. *AIMS Math* 8: 19677–19698. https://doi.org/10.3934/math.20231003

31. Xu C, Mu D, Liu Z, et al. (2023) Bifurcation dynamics and control mechanism of a fractional–order delayed Brusselator chemical reaction model. *Match* 89: 73–106. https://doi.org/10.46793/match.89-1.073x

32. Ahmad I, Bakar AA, Ali A, et al. (2023) Computational analysis of time-fractional models in energy infrastructure applications. *Alex Eng J* 82: 426–436. https://doi.org/10.1016/j.aej.2023.09.057

33. Jan R, Alyobi S, Inc M, et al. (2023) A robust study of the transmission dynamics of malaria through non-local and non-singular kernel. *AIMS Math* 8: 7618–7640. https://doi.org/10.3934/math.2023382

34. Thabet STM, Abdo MS, Shah K, et al. (2020) Study of transmission dynamics of COVID-19 mathematical model under ABC fractional order derivative. *Results Phys* 19: 103507. https://doi.org/10.1016/j.rinp.2020.103507

35. Jan R, Khurshaid A, Alotaibi H, et al. (2023) A robust study of the transmission dynamics of syphilis infection through non-integer derivative. *AIMS Math* 8: 6206–6232. https://doi.org/10.3934/math.2023314

36. Caputo M (1967) Linear models of dissipation whose Q is almost frequency independent—II. *Geophys J Int* 13: 529–539. https://doi.org/10.1111/j.1365-246X.1967.tb02303.x

37. Atangana A, Baleanu D (2016) New fractional derivatives with nonlocal and non-singular kernel: theory and application to heat transfer model. *Therm Sci* 20: 763–769. https://doi.org/10.2298/TSCI160111018A

38. Delamater PL, Street EJ, Leslie TF, et al. (2019) Complexity of the basic reproduction number (R0). *Emerg Infect Dis* 25: 1–4. https://doi.org/10.3201/eid2501.171901

39. Toufik M, Atangana A (2017) New numerical approximation of fractional derivative with non-local and non-singular kernel: application to chaotic models. *Eur Phys J Plus* 132: 1–16. https://doi.org/10.1140/epjp/i2017-11717-0

40. Xu C, Cui X, Li P, et al. (2023) Exploration on dynamics in a discrete predator–prey competitive model involving feedback controls. *J Biol Dyn* 17: 2220349. https://doi.org/10.1080/17513758.2023.2220349

41. Mua D, Xub C, Liua Z, et al. (2023) Further insight into bifurcation and hybrid control tactics of a chlorine dioxide–iodine–malonic acid chemical reaction model incorporating delays. *MATCH Commun Math Comput Chem* 89: 529—566. https://doi.org/10.46793/match.89-3.529M

42. Xu C, Cui Q, Liu Z, et al. (2023) Extended hybrid controller design of bifurcation in a delayed chemostat model. *MATCH Commun Math Comput Chem* 90: 609–648. https://doi.org/10.46793/match.90-3.609X

43. Ou W, Xu C, Cui Q, et al. (2023) Mathematical study on bifurcation dynamics and control mechanism of tri-neuron bidirectional associative memory neural networks including delay. *Math Methods Appl Sci* 2023: 1–25. https://doi.org/10.1002/mma.9347